Response to Review C

Thank you for your thoughtful and helpful review of our paper. It has helped us to craft a more precise and readable paper. Below we list your comments (in red) and our responses (in black).

The authors conclude that the primary cause of inter-model differences in MHTmax is atmospheric, involving the simulation of clouds. But if differences in ocean components were leading to different amounts of ocean heat transport, and thereby to different amounts of MHTmax, how would the methodology detect this? Since the equations the authors present are correct, there must be a reasonable answer to this question. (Perhaps it involves OLR variation with latitude.) But the text needs to address the question, lest casual readers conclude that by definition the ocean is a slave of the atmosphere.

The reviewer is correct to point out that our methodology, presented in this manuscript, does NOT distinguish between energy transports in the atmosphere and the ocean. We have added caveats to our conclusions in Section 3 to emphasize this point:

"We emphasize that, although the inter-model spread in MHT_{MAX} is (radiatively) due to difference in shortwave reflection within the atmosphere, the inter-model differences in the dynamic transports (the circulations that transport the energy) can be in either the atmosphere or the ocean (see Conclusion section for further discussion on this point)."

From the radiative perspective, both atmospheric and oceanic energy transports impart their signatures on the TOA radiative fields by ameliorating the equator-to-pole gradient in OLR (decreasing OLR*). For example, in the purely radiative limit, the system would be in local (latitude band by latitude band) radiative equilibrium and ASR* and OLR* would be equal – call this result OLR^*_{RAD}. If either the oceanic or atmospheric heat transport were turned on, the convergence of energy in the extratropics would increase the temperature, thereby reducing OLR* (relative to OLR^*_{RAD}) by an amount equal to MHT_{MAX} (in either the ocean or the atmosphere); in order to balance the dynamic heat transport, the extratropics must export an equal amount of radiation to space relative to the radiative expectation. This result is independent of whether the energy transport is in the atmosphere or the ocean. We have incorporated a (shortened) discussion of these points into the conclusion section.

The contribution of the atmospheric and oceanic heat transports to the inter-model spread in MHT_{MAX} can be formally separated by analyzing the surface and atmospheric energy budgets separately. We have performed this analysis but decided not to include it in the manuscript in order to keep the manuscript focused and of reasonable length. We have incorporated a brief discussion of the results in the conclusion section of the revised manuscript. We also provide those results for your interest below.

In steady state, the net energy flux through the ocean surface must be balanced by ocean heat transport convergence. We exploit this balance to separate the meridional heat transport in each of the CMIP3 PI simulations into oceanic and atmospheric contributions

(Fig. C1). There is substantial inter-model spread in both the oceanic and atmospheric energy transports, peaking in the regions of maximum heat transport around (20^o in the ocean an 40^o in the atmosphere). At the latitude of maximum total heat transport, there is approximately twice as much inter-model spread in the atmospheric energy transport than the oceanic energy transport. We partition MHT_{MAX} into atmospheric and oceanic components in each model (defined as the respective contributions to the heat transport at the latitude of MHT_{MAX}). The regression coefficient between total MHT_{MAX} and the atmospheric contribution is approximately twice as large as that with the oceanic contribution (Fig. C2). This result suggests that differences in atmospheric heat transport account for the majority of the differences in total MHT_{MAX}.

Two additional minor complaints: (1) The Abstract needs to make it clear that all the work presented here is based on annual means.

Fixed.

(2) Observational error estimates are needed in Table 3 and error bars in several figures -- or at least a discussion in the text that's more extensive than the footnote and single reference on Page 8. Other good references on observational errors are Trenberth and Fasullo, JPO 2008 Fig. 9; Fasullo and Trenberth, J Climate 2008 Fig. 7(d); Wunsch and Heimbach, JPO 2009 Fig. 6; Zheng and Giese, JGR 2009 Fig. 1(a).

We have attempted to project observational errors in the CERES radiative fields onto the quantities calculated in the manuscript. Such a calculation depends critically on the nature of the errors (Wunsch 2006) and any calculation requires assumptions about the magnitude of the errors, both systematic and random, and the decorrelation spatial scale of the errors. The true nature of the errors have not been adequately assessed by the research community (Carl Wunsch, personal communication) and are beyond the scope of the present work; we believe giving quantitative error bounds would do a disservice to the community because the assumptions made in such calculations and the sensitivity of the error bounds to those assumptions have not been adequately studied. None the less, we provide our error estimates below. We have also added a more thorough discussion of the likely error bounds and appropriately caveated any comparison between the models and the observations in out revised manuscript.

We use the CERES absolute calibration errors of 2% for shortwave fluxes and 1.5% for longwave fluxes (Loeb et al., 2009) in a Monte-Carlo simulation to project errors onto MHT_{MAX}, ASR*, and OLR*. In each of 1000 Monte-Carlo simulations, the zonal mean upwelling and downwelling SW fluxes at the TOA and the OLR are each multiplied by a randomly sampled factor from a distribution with a mean of one and a standard deviation of 0.020 and 0.015 respectively. *We explicitly assume that the errors at each latitude band are uncorrelated with the errors at adjacent latitude bands (and beyond)*. If the decorrelation spatial scale of errors is larger than one latitude band (it most likely is) then our calculations represent a lower bound on the observational uncertainty of ASR*, OLR* and MHT_{MAX} (because random errors will tend to cancel out when integrated over the extratropical regions if the decorrelation length scale is small but not if the

decorrelation length scale is large). The mean ASR*, OLR*, and MHT_{MAX} values of the 1000 simulations are statistical indistinguishable from the values reported in the manuscript. The error bars on ASR*, OLR* and, MHT_{MAX} are defined as 2.6σ of the Monte-Carlo ensemble, representing the one sided range of the 99% confidence interval (Table C1).

(PW)	MHT_{MAX}	ASR*	OLR*	incident	ASR* net albedo	ASR* surf	ASR* atmos
NH	0.31	0.25	0.19	0.16	0.11	0.02	0.11
SH	0.31	0.25	0.18	0.17	0.11	0.01	0.11

Table C1. The observational error bounds on the quantities calculated in the manuscript. The error bounds are taken as 2.6σ of the Monte-Carlo simulation as described in the text of this review response.

We also calculate the incident and net albedo contributions to ASR* as defined in the manuscript for each Monte-Carlo members. The net albedo contribution to ASR* is further subdivided into atmospheric and surface contributions by propagating the net albedo ASR* error onto $ASR*_{SURF}$ and $ASR*_{ATMOS}$ through the use of the planetary albedo partitioning error estimates described by Donohoe and Battisiti (2011) in Appendix B. In this case, both the uncertainty in the net albedo contribution to ASR* and the uncertainty in the partitioning of planetary albedo into atmospheric and surface components contribute to the errors in $ASR*_{SURF}$ and $ASR*_{ATMOS}$. The errors on all quantities scale linearly with their climatological values with errors in ASR* and OLR* adding in quadrature to errors in MHT_{MAX} (not shown). This result is unsurprising given that we assumed at the outset that longwave, and upweliing and downweliing shortwave fluxes scaled as a percent of the climtological flux and were independent of eachother.

Our error estimates are significantly smaller (by a factor of two or three) than those of Wunsch (2006). The discrepancy most likely stems from differences in the decorrelation length scale of the errors. Further investigation is underway.

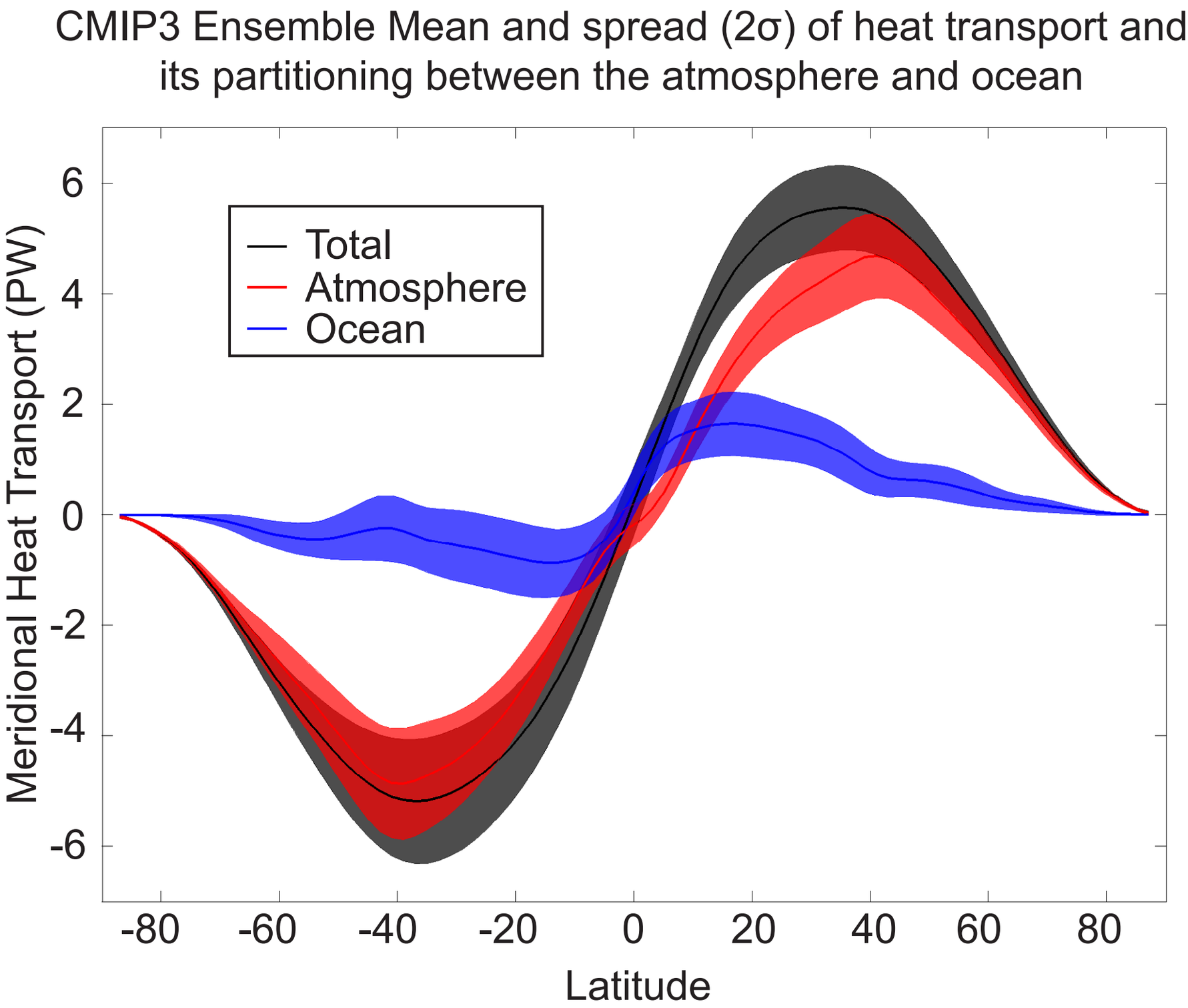

Fig. C1. The CMIP3 PI inter-model mean (dark lines) and inter-model spread (2σ -- shading) of meridional heat transport (in PW). The total (black) is seperated into atmospheric (red) and oceanic (blue) contributions.

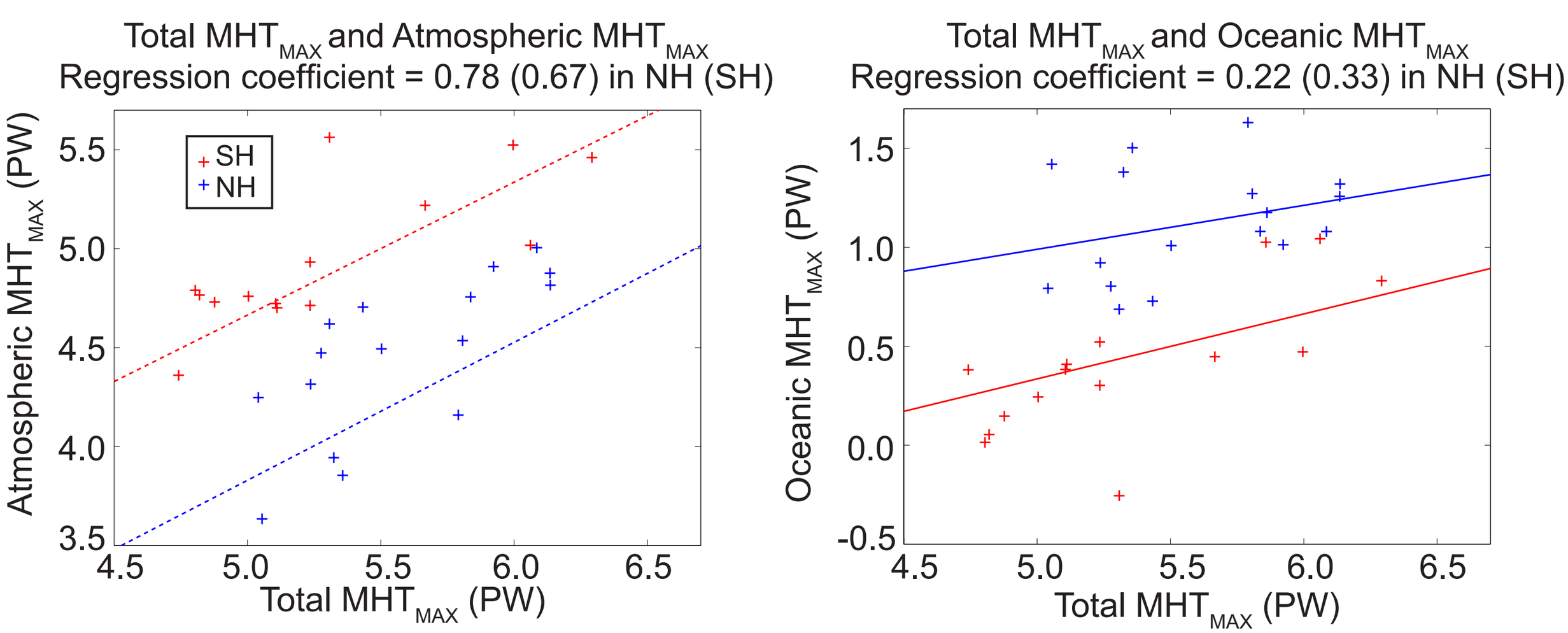

Fig C2. (A) Atmospheric contribution to MHT_{MAX} and (B) oceanic contribution to MHT_{MAX} versus total MHT_{MAX} in the CMIP3 PI ensmble. The red crosses represent the SH and the blue crosses represent the NH with each cross corresponding to a different model. The dashed lines are the linear best fits of the inter-model differences. (C) Summary of the spread (2σ) in MHT_{MAX} divided into the part that is linearly congruent with the atmospheric and oceanic contributions (defined as the regression coefficients in (A) and (B) times the inter-model spread in MHT_{MAX}).